

# RSC Advances



This is an *Accepted Manuscript*, which has been through the Royal Society of Chemistry peer review process and has been accepted for publication.

*Accepted Manuscripts* are published online shortly after acceptance, before technical editing, formatting and proof reading. Using this free service, authors can make their results available to the community, in citable form, before we publish the edited article. This *Accepted Manuscript* will be replaced by the edited, formatted and paginated article as soon as this is available.

You can find more information about *Accepted Manuscripts* in the [Information for Authors](#).

Please note that technical editing may introduce minor changes to the text and/or graphics, which may alter content. The journal's standard [Terms & Conditions](#) and the [Ethical guidelines](#) still apply. In no event shall the Royal Society of Chemistry be held responsible for any errors or omissions in this *Accepted Manuscript* or any consequences arising from the use of any information it contains.

Cite this: DOI: 10.1039/c0xx00000x

www.rsc.org/xxxxxx

ARTICLE TYPE

# Molecular packing, crystal to crystal transformation, electron transfer behaviour, photochromic and fluorescent property of three hydrogen-bonded supramolecular complexes containing benzenecarboxylate donors and viologen acceptors

Hengjun Chen,<sup>a</sup> Min Li,<sup>a</sup> Guiming Zheng,<sup>a</sup> YiFang Wang,<sup>a</sup> Yang Song,<sup>a</sup> Conghui Han,<sup>a</sup> Zhiyong Fu<sup>\*a</sup>  
Shijun Liao,<sup>a</sup> and Jingcao Dai<sup>b</sup>

Received (in XXX, XXX) Xth XXXXXXXXX 20XX, Accepted Xth XXXXXXXXX 20XX

DOI: 10.1039/b000000x

An investigation into the relation between structures of three D-A supramolecular systems and their photoresponsive characteristics is presented. Compound **1** [H<sub>2</sub>CPBPY]·[H<sub>2</sub>BTEC] and compound **2** [HCPBPY]<sub>2</sub>·[H<sub>2</sub>BTEC]·5H<sub>2</sub>O are prepared with the same starting materials at different pH values and characterized by single crystal X-ray diffraction, powder X-ray diffraction, UV-vis, IR and ESR spectra. Electron-deficient CPBPY moieties and electron-donating BTEC units are linked by hydrogen-bonds and  $\pi$ - $\pi$  stacking interactions to form the donor-acceptor systems. Under light irradiation, photoactivated electrons can transfer from the donor to the acceptor units in both **1** and **2**, giving rise to a long-lived charge-separated state and accompanying an interesting color changing phenomenon. Crystals of **2** allowed to dehydrate at elevated temperature undergo single-crystal to single-crystal transformation to yield **3** [HCPBPY]<sub>2</sub>·[H<sub>2</sub>BTEC], accompanied by a drastic change in structural arrangements. For the photocoloration character, compound **1** shows a faster photoresponsive rate than **2** and **3**. For the fluorescence property, compound **1** and **2** both exhibit photoluminescence emission centered at 400 nm, whereas **3** exhibits photoluminescence emission at 520 nm, showing a significant red shift of 120 nm. Their different photoactive characters can be attributed to the connecting, packing modes and the valence states of the functional D-A moieties.

Investigating the self-assembly of electron donor (D) and acceptor (A) units and the mechanism of photoinduced electron transfer (PET) process is of primary importance in constructing functional molecular devices that can convert solar energy into useful chemical energy.<sup>1</sup> It is known that electron transfer could take place in a well-organized D-A molecular system under light irradiation. Over the past few decades, numerous photosensitive smart molecular systems have been explored with the combination of the D-A units, such as the assembly of porphyrin-fullerene,<sup>2</sup> porphyrin-quinone,<sup>3</sup> phthalocyanine-SWNTs,<sup>4</sup> H<sub>4</sub>DPP<sup>2+</sup>-fcCOOH,<sup>5</sup> crown ether-viologen,<sup>6</sup> pyrene-viologen,<sup>7</sup> Ru(bpy)<sub>3</sub>-viologen,<sup>8</sup> ZnP-viologen units.<sup>9</sup> Recently, novel D-A systems were created under the direction of supramolecular crystal engineering in which donors and acceptors are aggregated *via* non-covalent interactions. This synthesis strategy can not only avoid tedious synthesis but also provide chances for obtaining D-A complexes with multiple crystal structures that may lead to different photo-responsive properties.<sup>10-12</sup> The self-assembly of synthons involving organic  $\pi$  systems has been revealed as an effective strategy to build p-type or n-type photoelectric materials.<sup>13</sup> Multitude of individual molecules with electron donor and electron acceptor functionalities are organized through hydrogen-bonds and  $\pi$ - $\pi$  stacking intermolecular interactions.<sup>14</sup>

Besides their structure-directing role, noncovalent forces also contribute to enhance electronic interactions between D-A fragments and pave the road for electron transfer.<sup>11a</sup> After the electron transfer reactions, stable charge-separated state can be retained in crystalline materials for a long time.<sup>15,16</sup> And interesting photochromic phenomena deriving from the formation of radicals are also observed at the same time. Photochromic materials can change their color under light stimuli, which are considered as excellent candidates for optical information storage and fluorescent switches.<sup>17,18</sup> Fabricating the array of the electron donor and acceptor units controllably within photosensitive materials at a molecular level is critical for the development of new optoelectronic devices.<sup>19</sup> However, a systematic investigation into the structure-property relationship of the noncovalent assembled donor-acceptor motifs is still limited. Considering crystal engineering is an efficient approach to manipulate the arrangement of electron donor and acceptor units, we have embarked on a program to investigate the relation between photoresponsive characters and interactions of D-A blocks by taking advantage of supramolecular assembly. Herein, we report the syntheses and stimuli-responsive properties of three BTEC-CPBPY complexes, namely [H<sub>2</sub>CPBPY]·[H<sub>2</sub>BTEC] (**1**), [HCPBPY]<sub>2</sub>·[H<sub>2</sub>BTEC]·5H<sub>2</sub>O (**2**) and [HCPBPY]<sub>2</sub>·[H<sub>2</sub>BTEC] (**3**)

(BTEC = benzenetetracarboxylate, CPBPY = N-(3-carboxyphenyl)-4,4'-bipyridinium). The pH values of the reaction systems result in the different structural self-assemblies of **1** and **2**. Compound **2** exhibits an interesting single-crystal to single-crystal transformation upon heating at 130 °C into a dehydrated form (compound **3**). And the space group of its crystalline form changes from P-1 to P2<sub>1</sub>/c after the removal of the water molecules. In contrast with **2**, compound **3** adopts a more close-packed structure. Deriving from the D-A electron transfer process, the crystals of these three complexes all change their color from yellow to green on account of the formation of long-lived radicals. Among them, **1** shows a higher photoresponsive rate. Compound **1** and **2** both exhibit fluorescence emission at 400 nm, whereas **3** exhibits fluorescence emission at 520 nm, showing a significant red shift of 120 nm. Distance, orientation and interactions, packing mode and the protonation degree of the assembly units are important factors in affecting the photoactive characters.

## Experimental section

### 1. General methods and materials

All the reagents were purchased from commercial sources and used without further purification. N-(3-carboxyphenyl)-4,4'-bipyridinium chloride was synthesized as reported.<sup>20</sup> ATA instrument Q600 SDT thermogravimetric analyzer was used to obtain the TGA curve in N<sub>2</sub> at a rate of 10 °C min<sup>-1</sup>. The X-ray powder diffraction (XRD) data were collected with a Bruker D8 Advance X-ray diffractometer using CuK $\alpha$  radiation ( $\lambda = 1.5406$  Å). UV-Visible spectral measurements were carried out using a HITACHI U-3010 spectrometer. IR spectra were characterized by a Bruker Tensor 27 FTIR spectrometer in the range of 4000–400 cm<sup>-1</sup> using a KBr disk. The ESR spectra were recorded at room temperature with a Bruker EMX-10/12 electron spin resonance spectrometer. The C, H and N microanalyses were carried out with a Vario EL III elemental analyzer.

### 2. Syntheses of compound **1**, **2** and **3**

**1:** N-(3-carboxyphenyl)-4,4'-bipyridinium chloride (0.0463 g, 0.15 mmol) was added to a mixed solution containing 1,2,4,5-benzenetetracarboxylic acid (0.0508 g, 0.2 mmol), DMF (2 mL), C<sub>2</sub>H<sub>5</sub>OH (4 mL) and H<sub>2</sub>O (4 mL). The mixture was stirred in a 25 mL beaker for 10 min. After a week, yellow needle-like crystals were collected by filtration, washed with water, and dried at room temperature (0.089 mmol, 0.0475 g, 59.3% yield based on HCPBPY. IR (KBr):  $\nu = 3489$  (s), 3420 (s), 3398 (s), 3112 (m), 3033 (m), 2969 (m), 2918(m), 2861 (m), 2839 (m), 1703(s), 1629(s), 1560 (s), 1498 (s), 1355 (s), 1287 (s), 1173 (s), 1150 (s), 1092 (s), 979 (m), 859 (w), 807 (m), 761 (s), 699 (m), 596 (m) cm<sup>-1</sup>. Anal. C<sub>27</sub>H<sub>18</sub>N<sub>2</sub>O<sub>10</sub> (530.43) (%): calcd. C 61.14, H 3.42, N 5.28; found C 60.15, H 3.33, N 5.28.

**2:** N-(3-carboxyphenyl)-4,4'-bipyridinium chloride (0.0463 g, 0.15 mmol) was added to a mixed solution containing 1,2,4,5-benzenetetracarboxylic acid (0.0508 g, 0.2 mmol), DMF (2 mL), C<sub>2</sub>H<sub>5</sub>OH (4 mL), H<sub>2</sub>O (2 mL) and NaOH (2 mL, 0.1 M). The mixture was stirred in a 25 mL beaker for 10 min. After a week, yellow block-shape crystals were collected by filtration, washed with water, and dried at room temperature (0.089 mmol, 0.0398 g, 58.6% yield based on HCPBPY. IR (KBr):  $\nu = 3446$  (s), 3089

(m), 1697 (s), 1635 (s), 1560 (s), 1486 (s), 1361 (s), 1270 (s), 1207 (s), 1178 (s), 1104 (s), 1064 (s), 1013 (m), 871 (w), 825 (s), 761 (s), 716(s), 631(m) cm<sup>-1</sup>. Anal. C<sub>44</sub>H<sub>40</sub>N<sub>4</sub>O<sub>17</sub> (896.80) (%): calcd. C 58.93, H 4.50, N 6.25; found C 58.90, H 4.29, N 6.25.

**3:** Compound **3** was obtained by heating compound **2** in an oven at 130 °C for 2 hours in the air. No notable changes in the appearance of the crystal was observed after the single-crystal to single-crystal transformation. IR (KBr):  $\nu = 3122$  (m), 3087 (m), 3010(m), 2247(m), 1930(m), 1703 (s), 1633 (s), 1589 (s), 1411 (s), 1338 (s), 1292 (s), 1058 (s), 1010 (s), 825 (s), 763 (s), 717(s) cm<sup>-1</sup>. Anal. C<sub>22</sub>H<sub>15</sub>N<sub>2</sub>O<sub>6</sub> (403.36) (%): calcd. C 65.50, H 3.748, N 6.945; found C 64.59, H 3.657, N 6.776.

### 3. Crystal Structure Determination

The measurements were taken on a Rigaku R-Axis SPIDER CCD diffractometer with graphite-Monochromated Mo/K $\alpha$  radiation. Data were collected at 298K, using the  $\omega$ - and  $\phi$ -scans to a maximum  $\theta$  value of 25.03°. The data were refined by full-matrix least-squares techniques on F<sup>2</sup> with SHELXTL-97.<sup>21</sup> And the structures were solved by direct methods SHELXS-97.<sup>22</sup> All non-hydrogen atoms were refined anisotropically. The hydrogen atoms on the oxygen atoms of the carboxyl groups and the nitrogen atoms of the CPBPY molecules are located from difference Fourier mapping. Other hydrogen atoms were included at geometrically idealized positions.

#### Crystal data for **1**

C<sub>27</sub>H<sub>18</sub>N<sub>2</sub>O<sub>10</sub>,  $f_w = 530.43$  g·mol<sup>-1</sup>, Monoclinic, space group C2/c,  $a = 26.032(7)$  Å,  $b = 8.8150(15)$  Å,  $c = 21.444(8)$  Å,  $\alpha = 90^\circ$ ,  $\beta = 110.25(3)^\circ$ ,  $\gamma = 90^\circ$ ,  $V = 4617(2)$  Å<sup>3</sup>,  $Z = 8$ ,  $\rho_{\text{calcd}} = 1.526$  g·cm<sup>-3</sup>,  $\mu = 0.119$ ,  $F(000) = 2192$ ,  $\text{GoF} = 1.061$ , final  $R_I = 0.0424$  and  $wR_2 = 0.1124$  for 2922 independent reflections [ $I > 2\sigma(I)$ ].

#### Crystal data for **2**

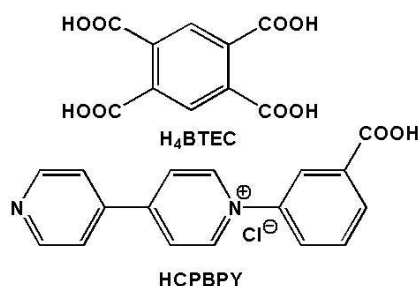
C<sub>44</sub>H<sub>40</sub>N<sub>4</sub>O<sub>17</sub>,  $f_w = 896.80$  g·mol<sup>-1</sup>, Triclinic, space group P-1,  $a = 7.3700(15)$  Å,  $b = 9.5200(19)$  Å,  $c = 15.776(3)$  Å,  $\alpha = 90.26(3)^\circ$ ,  $\beta = 102.68(3)^\circ$ ,  $\gamma = 106.00(3)^\circ$ ,  $V = 1035.6(4)$  Å<sup>3</sup>,  $Z = 1$ ,  $\rho_{\text{calcd}} = 1.438$  g·cm<sup>-3</sup>,  $\mu = 0.112$ ,  $F(000) = 468$ ,  $\text{GoF} = 1.073$ , final  $R_I = 0.0396$  and  $wR_2 = 0.0890$  for 2241 independent reflections [ $I > 2\sigma(I)$ ].

#### Crystal data for **3**

C<sub>22</sub>H<sub>15</sub>N<sub>2</sub>O<sub>6</sub>,  $f_w = 403.36$  g·mol<sup>-1</sup>, monoclinic, space group P2<sub>1</sub>/c,  $a = 8.9819(18)$  Å,  $b = 12.923(3)$  Å,  $c = 15.042(3)$  Å,  $\alpha = 90^\circ$ ,  $\beta = 97.40(3)^\circ$ ,  $\gamma = 90^\circ$ ,  $V = 1731.4(6)$  Å<sup>3</sup>,  $Z = 4$ ,  $\rho_{\text{calcd}} = 1.548$  g·cm<sup>-3</sup>,  $\mu = 0.115$ ,  $F(000) = 836$ ,  $\text{GoF} = 1.025$ , final  $R_I = 0.0441$  and  $wR_2 = 0.1008$  for 1816 independent reflections [ $I > 2\sigma(I)$ ].

## Results and discussion

The reasons for choosing BTEC as the donor and CPBPY as the acceptor is based on the following considerations: (1) viologens are classic electron-deficient molecules that can receive electron to form radicals<sup>23</sup> and benzenecarboxylates are widely used as electron donating components<sup>24</sup>; (2) The D-A system can be easily constructed in a simple way that avoids the inconvenient organic synthesis and purification process. The carboxyl groups of H<sub>4</sub>BTEC tend to bond with the pyridine and the carboxyl groups of CPBPY in either hydrogen-bond or salt bridge manners.



**Scheme. 1** Chemical structure of  $\text{H}_4\text{BTEC}$  and  $\text{HCPBPY}$

Moreover, they are both  $\pi$ -electron rich molecules that can adopt a close packing mode *via*  $\pi$ - $\pi$  stacking interactions; (3) Both BTEC and CPBPY are possible to exhibit various valence state results from the deprotonation of carboxyl groups and the protonation of pyridine groups. The valence states of the donor and acceptor units can impact the electron transfer behavior and the photochromism of the final assembled networks.

### Structure of $[\text{H}_2\text{CPBPY}] \cdot [\text{H}_2\text{BTEC}]$ (1)

Compound **1** is prepared in an acidic solution (pH = 3.26). X-ray crystal diffraction analysis reveals the formation of a mixed-stacking structure constructed by  $[\text{H}_2\text{CPBPY}]^{2+}$  and  $[\text{H}_2\text{BTEC}]^{2-}$  building blocks. As shown in Fig. 1a, the viologen-based block receives one proton to serve as a bivalent cation. The benzenetetracarboxylic acid molecule deprotonates two protons, forming a bivalent anion. A strong hydrogen-bond joining the pyridine end of  $\text{H}_2\text{CPBPY}$  and the carboxyl group of the adjacent  $\text{H}_2\text{BTEC}$  molecule is observed ( $\text{N-H}\cdots\text{O} = 2.676 \text{ \AA}$ ). Hydrogen-bonds connecting the carboxyl groups of  $[\text{H}_2\text{CPBPY}]^{2+}$  and  $[\text{H}_2\text{BTEC}]^{2-}$  are also observed ( $\text{O-H}\cdots\text{O} = 2.592 \text{ \AA}$ ). The donors and acceptors are then assembled to build a twisted supramolecular chain by the hydrogen-bond connections of  $\text{N-H}\cdots\text{O}$  and  $\text{O-H}\cdots\text{O}$  manners in a  $\cdots\text{DADADA}\cdots$  order. Each  $\text{H}_2\text{CPBPY}$  molecule is surrounded by six  $\text{H}_2\text{BTEC}$  molecules. The distances from the carboxyl groups to the central pyridinium

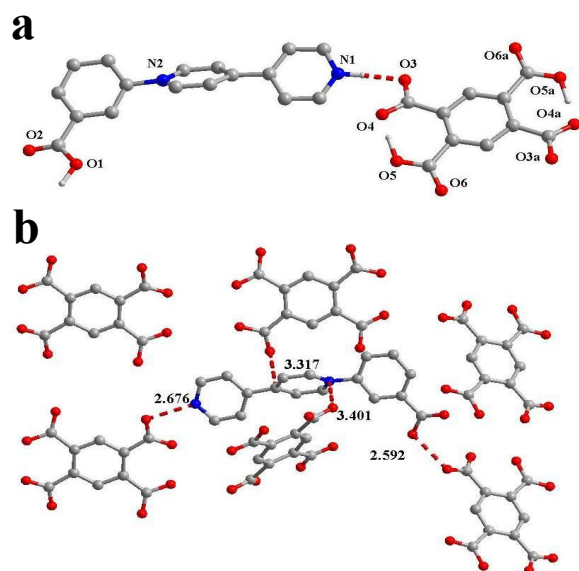


**Fig. 1** Molecular structure of compound **1**: (a) the asymmetric structural unit; (b) diagram to show the distances between the D-A units.

ring vary from  $3.317 \text{ \AA}$  to  $3.401 \text{ \AA}$  (Fig. 1b). The supramolecular chains interweave with each other by  $\pi$ - $\pi$  stacking interactions, which increase the chances of intermolecular electron transfer and finally extend the structural motif to a 3D supramolecular network (Fig. S1, see ESI<sup>†</sup>).

### Structure of $[\text{HCPBPY}]_2 \cdot [\text{H}_2\text{BTEC}] \cdot 5\text{H}_2\text{O}$ (2)

With the same starting materials, compound **2** is obtained in a slightly more basic condition (pH = 4.18). Single crystal data display that the asymmetric unit of **2** is made up of  $\text{HCPBPY}$ ,  $\text{H}_2\text{BTEC}$  and lattice water molecules (Fig. 2a). Unlike compound **1**, the viologen molecule remains its original form as a monovalent cation. Each  $\text{HCPBPY}$  molecule neighbors with three  $\text{HCPBPY}$  molecules and three  $\text{H}_2\text{BTEC}$  molecules.  $\pi$ - $\pi$  interactions are observed between the adjacent  $\text{HCPBPY}$  molecules in a face to face alignment ( $3.715 \text{ \AA}$ ). The carboxyl group of  $\text{H}_2\text{BTEC}$  molecule generates two hydrogen-bonds with the nearby carboxyl groups from other two  $\text{H}_2\text{BTEC}$  molecules,

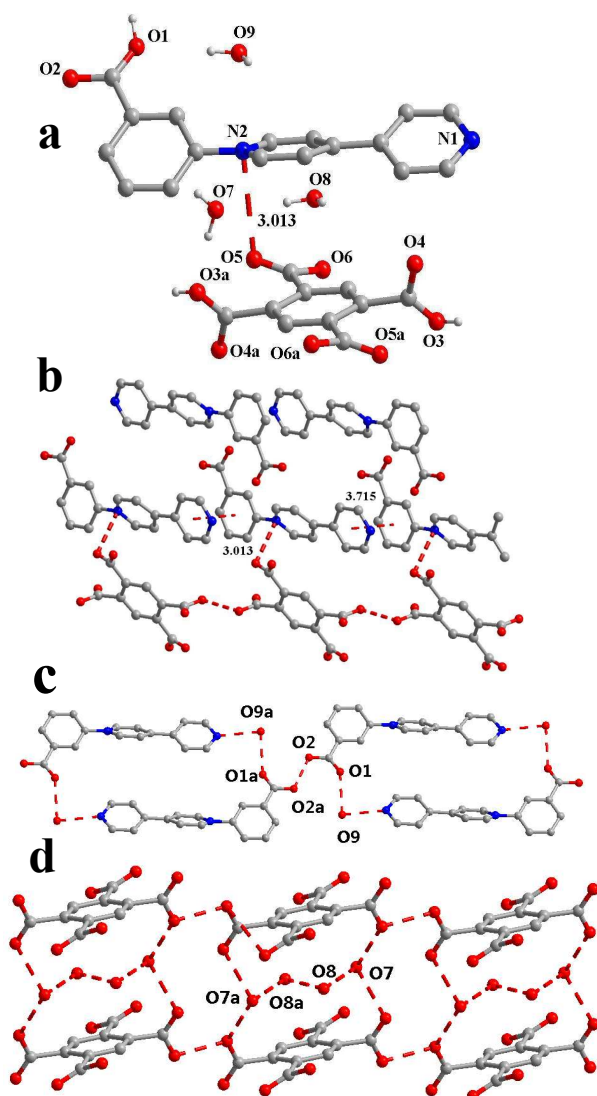


**Fig. 2** Molecular structure of compound **2**: (a) the asymmetric structural unit; (b) diagram to show the distances between the D-A units; (c) the hydrogen-bonded network of the lattice water molecules and  $\text{HCPBPY}$  cations; (d) the hydrogen-bonded network of the lattice water molecules and  $\text{H}_2\text{BTEC}$  anions.

which continue to join the neighbouring molecules to form a 1D supramolecular chain. The distance between the carboxyl groups of the H<sub>2</sub>BTEC chain and the pyridinium rings of the HCPBPY chain is 3.013 Å, in which electrons can transfer from the donor to the acceptor moieties favorably (Fig. 2b). Five water molecules are included into the lattice. The carboxyl of one HCPBPY cation and the pyridine N of another HCPBPY cation are hydrogen-bonded with one water molecule node (O9) to yield a HCPBPY chain (Fig. 2c). The other four water molecules are connected with the adjacent ones to form a (H<sub>2</sub>O)<sub>4</sub> cluster, which is clipped by two H<sub>2</sub>BTEC molecules. The connections between the (H<sub>2</sub>O)<sub>4</sub> cluster and H<sub>2</sub>BTEC molecules through noncovalent forces generate a ...H<sub>2</sub>BTEC-(H<sub>2</sub>O)<sub>4</sub>-H<sub>2</sub>BTEC... network (Fig. 2d). The HCPBPY chains and the H<sub>2</sub>BTEC-water networks are bound by hydrogen-bonds *via* the water molecule node (O9) to give rise to a 3D supramolecular assembly (Fig. S2, see ESI†).

### Structure of [HCPBPY]<sub>2</sub>·[H<sub>2</sub>BTEC] (3)

Light and heat activate the reversible photochromic transformation of these D-A complexes in solid state. As **2** is a pentahydrate complex, it is necessary to investigate its thermal behavior. Interestingly, crystals of **2** undergo an irreversible transformation to yield **3** when heated at 130 °C for 2 hours. This process shows no obvious changes in the appearance of the sample. Single-crystal X-ray crystallographic analysis reveals that all lattice water molecules are removed from the structure. And the space group of **2** changes from P-1 to P2<sub>1</sub>/c for **3**. The structural transformation results in rearrangement of the D-A building blocks. The distances between the carboxyl groups and the pyridinium vary from 3.393 Å to 3.525 Å. Each H<sub>2</sub>BTEC molecule is surrounded by four HCPBPY molecules and they are hydrogen-bonded in O-H...N (O-H...N = 2.650 Å) and O...H-O manners (O...H-O = 2.476 Å) to build up a 2D supramolecular network. Finally, the 2D nets interweaves with each other by π-π

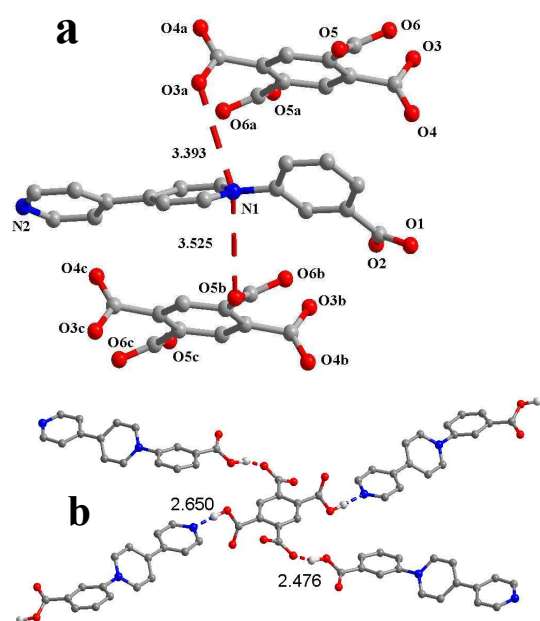


**Fig. 3** Molecular structure of compound **3**: (a) the asymmetric structural unit; (b) diagram to show the distances between D, A units.

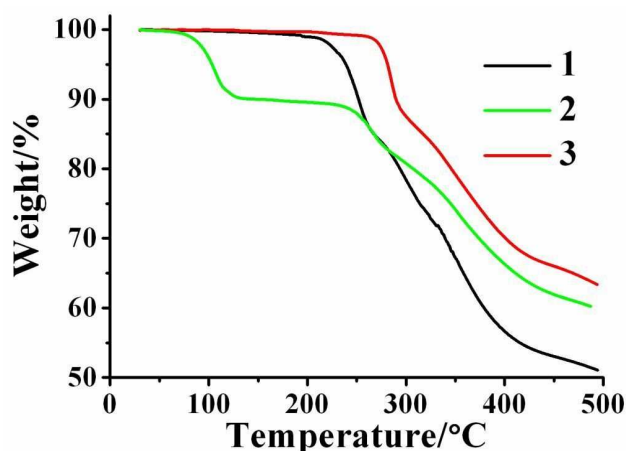


**Fig. 4** The TGA diagram for the three D-A complexes.

stacking forces to generate a dense packing network with a shortest distance of 3.502 Å between the adjacent supramolecular nets. (Fig. S3, see ESI†).

### TG, IR and XRD data

Thermogravimetric analyses (TGA) are performed on polycrystalline samples of these three compounds to investigate their thermal stability (Fig. 4). For **1**, an obvious decomposition was observed at 220 °C, corresponding to the destruction of the supramolecular framework. For **2**, two clean and well-separated weight loss steps are observed. It gives an obvious weight loss 9.99% in the first region (90-120 °C), suggesting the removal of five lattice water molecules per formula unit (calc. 10.03%). After the first weight loss, the TG curve of compound **2** are similar to that of compound **3**, which supports the result of the crystal transformation.

The IR spectrum of **1** shows the presence of a characteristic N-H stretching band at 3489 cm<sup>-1</sup>, confirming the protonation of the pyridine ring in H<sub>2</sub>CPBPY molecule (Fig. S4, see ESI†). The sharp peaks around 3420 cm<sup>-1</sup> and 3398 cm<sup>-1</sup> can be assigned to the O-H bonds of H<sub>2</sub>CPBPY and H<sub>2</sub>BTEC. A sharp carbonyl C=O peak for carboxylic acid is observed right around 1703 cm<sup>-1</sup>. For compound **2**, its IR spectrum shows broad bands centered at 3446 cm<sup>-1</sup> due to O-H stretches of lattice water. The peak at 1697 cm<sup>-1</sup> is C=O stretch. For compound **3**, the peak at 3446 cm<sup>-1</sup> disappear entirely, which supports the removal of water molecules. The band of O-H absorption occurring around 3100 cm<sup>-1</sup> is attributed to the strong hydrogen-bonding between the D-A units. And the peak at 1705 cm<sup>-1</sup> is the carbonyl stretching absorption. These data are well consistent with the results of the single crystal data.

The PXRD patterns of **1**, **2** and **3** are in good agreement with the simulated XRD-patterns obtained from single crystal data (Fig.S5, see ESI†). These results indicate that the bulk samples of them have high phase purity and crystallinity. No significant changes in the PXRD patterns of **3** are observed after either soaking the sample in water or placing it in a hot humid place, indicating the structural transformation is irreversible.

### UV-vis, ESR spectra, photocoloration and photoactivation-thermal cycles

The solid state photocoloration properties of these three complexes are studied by UV-Vis diffuse reflectance and ESR spectroscopy of microcrystalline powders. The UV-Vis spectra of **1**, **2** and **3** show intense bands near 345, 334 and 342 nm (Fig. 5), which are assigned to  $\pi$ - $\pi^*$  transitions of the aromatic moieties. Upon exposure to light irradiation (xenon lamp, 150 W), the pale-yellow powders of **1** turn green, giving rise to characteristic viologen radical bands at 417 nm and 666 nm, compound **2** gradually shift to yellow-green with the emerged absorption bands at around 462 nm and 674 nm, and compound **3** changes its

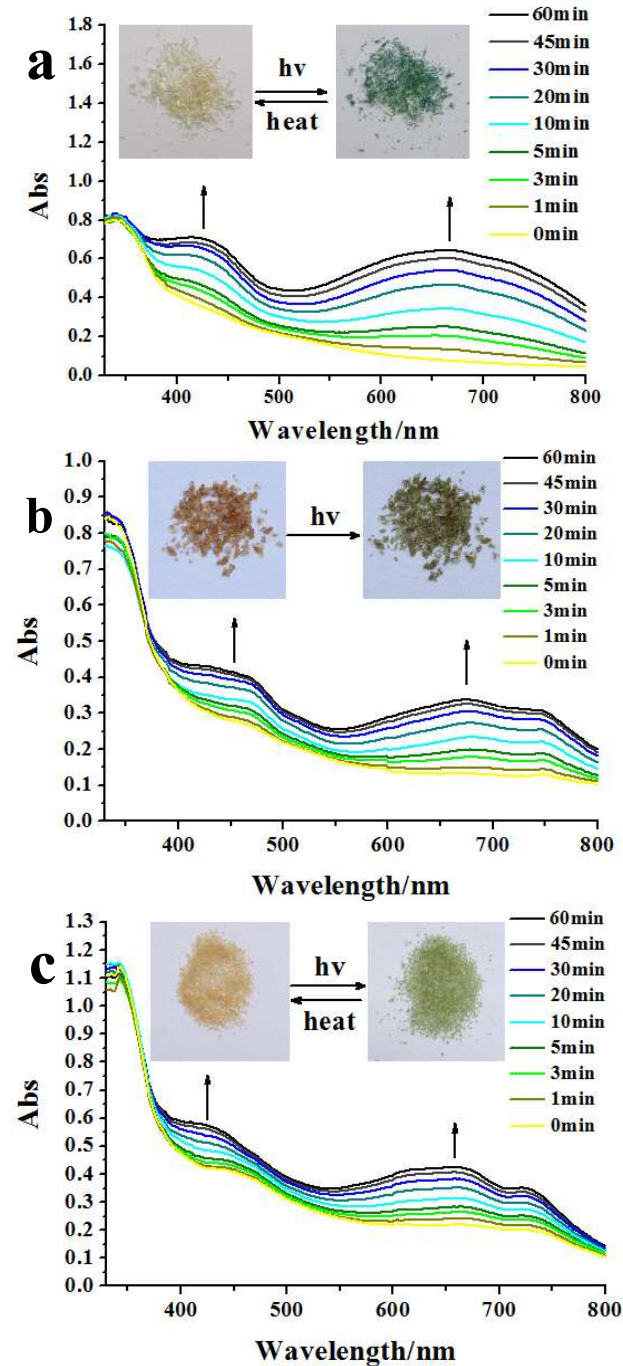


**Fig 5.** UV-vis spectral changes upon photo-irradiation: (a) compound **1**; (b) compound **2**; (c) compound **3**. Insets: Photographs of the crystals before and after photo-irradiation.

color to green with new absorption bands centered at 425 nm and 657 nm, with enhanced intensity as the irradiation time increases. The process of electron transfer and the generation of radicals of the titled three complexes are further confirmed by ESR measurements after photoirradiation under the same condition (compound **1**:  $g = 2.0020$ , compound **2**:  $g = 2.0019$  and compound **3**:  $g = 2.0018$ ) (Fig.S6, see ESI†). The  $g$  factors are consistent with the reported viologen radicals.<sup>25</sup> The mechanism of electron transfer from the carboxylate group, an extensively reported electron donor, to viologen-based electron acceptor has been well documented.<sup>26</sup> Single crystal data reveal that the distances between the pyridinium rings and the carboxyl groups are 3.317 Å, 3.013 Å and 3.393 Å for **1**, **2** and **3** respectively. These values are smaller than the threshold distance (3.5 Å) observed for light activated D-A systems, indicating a feasible environment for electron transfer.<sup>27</sup>

The character of reversible photoswitching is important for photochromic materials that can be applied as photoactive devices. Compound **1** and **3** both exhibit a bleaching phenomenon when they are heated at 130 °C in the air, the essence of which is a charge-recombination process.<sup>28</sup> Fig. 6 shows the switch between the charge-separated states and the ground state of these two complexes to five cycles by alternated irradiation and thermal treatment. The maximum absorbance peaks at 666 nm for **1** and 657 nm for **3** and the response time curve during bleaching all remain essentially unchanged.

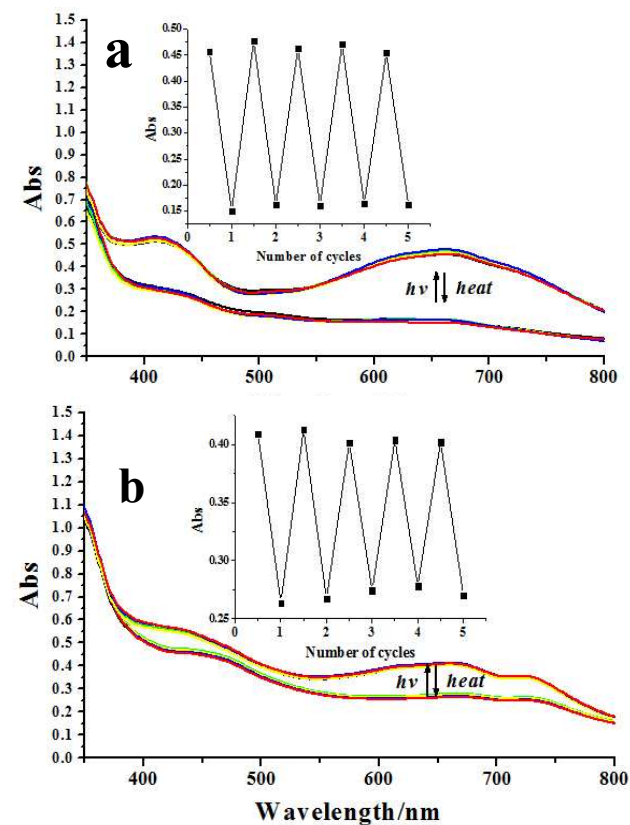


**Fig 6.** UV-vis spectral changes on alternate excitation by photoirradiation and heating over five cycles in the air: (a) compound **1**; (b) compound **3**. Insets: Variation of the absorbance at 666 nm for **1** and 657 nm for **3**.

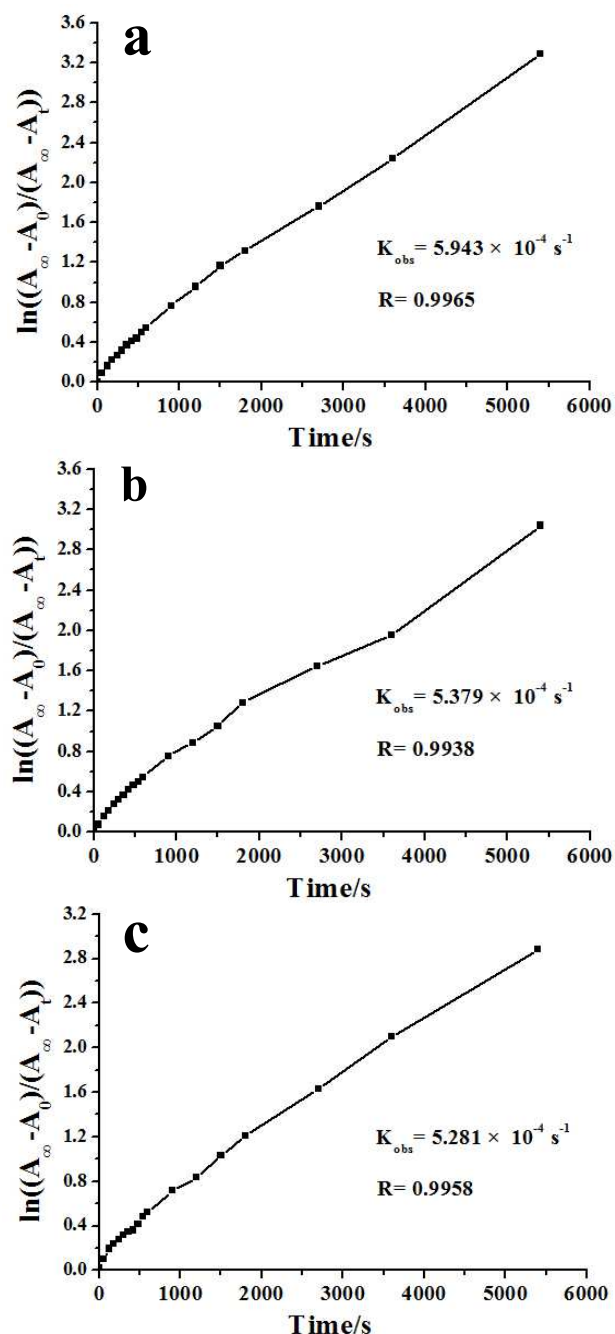


**Fig. 7** Solid state kinetic traces: photoinduced coloration based on UV absorption at (a) 666 nm for compound **1**; (b) 674 nm for compound **2**; (c) 657 nm for compound **3**.

#### Kinetic calculation

Kinetic calculation of photo-coloration of the title compounds is used to investigate their response rate to outer stimuli. Solid state light reversions of **1**, **2** and **3** followed at 666 nm, 674 nm and 657 nm all exhibit first order kinetics. They give the rate constant with  $k_{\text{obs}} = 5.943 \times 10^{-4} \text{ s}^{-1}$ ,  $k_{\text{obs}} = 5.379 \times 10^{-4} \text{ s}^{-1}$  and  $k_{\text{obs}} = 5.281 \times 10^{-4} \text{ s}^{-1}$  respectively (Fig. 7).

#### Correlation between the structure and the photosensitive property

The photosensitive properties of materials involving D-A units are known to be very sensitive to several factors such as unit interactions, the distance of the channel for electron transfer, the electron-accepting ability of the acceptor, and the electron-donating capability of the donor moiety.<sup>29</sup> In the same irradiation condition, compound **1** performs the fastest response rate and the highest extent of photoreaction ( $A_{60\text{min}}/A_{0\text{min}} = 8.27$ ) in comparison with compound **2** ( $A_{60\text{min}}/A_{0\text{min}} = 2.56$ ) and compound **3** ( $A_{60\text{min}}/A_{0\text{min}} = 1.93$ ). Investigation of their structures reveals that: (1) compound **1** is made up of bivalent cations [ $\text{H}_2\text{CPBPY}$ ] and bivalent anions [ $\text{H}_2\text{BTEC}$ ]. The pyridine ring of viologen unit is protonated and the benzenetetracarboxylic acid building block is deprotonated two protons. The higher ionic state of acceptor units increases the electric potential, thus facilitates the following photoactivated electron transfer reaction. Whereas, the photosensitive system of **2** and **3** is fabricated by the combination of monovalent cations [ $\text{HCPBPY}$ ] and bivalent anions [ $\text{H}_2\text{BTEC}$ ]. The stronger electron transfer tendency could be ascribed for the fastest reaction rate in **1**; (2) the D-A distance in **2** is 3.013 Å, whereas the value in **3** is 3.393 Å. Here, the distance of the channel for electron transfer may be the major determining factor for these two complexes, which leads to a slightly faster rate for **2** than **3**.

#### Fluorescent characters

Fig. 8 shows the fluorescent characters of these three D-A complexes in solid state. It can be observed that **1** and **2** all exhibit photoluminescence emission at 400 nm (Fig. 8a,  $\lambda_{\text{ex}} = 250$  nm), whereas **3** exhibits photoluminescence emission at 520 nm (Fig. 8b,  $\lambda_{\text{ex}} = 400$  nm). It is interesting to note that the emission wavelength of **3** is red shifted ( $\approx 120$  nm) with respect to those of **1** and **2**. Luminescence is known as sensitive to the mode of molecular packing in the solid state.<sup>30</sup> Intermolecular interactions, such as conformational changes,  $\pi$ - $\pi$  stacking and hydrogen-bonds etc., could induce rearrangements of the energy levels and population.<sup>31</sup> In compound **3**, the arrangement of the D-A blocks is changed with the structural transformation. It displays a more compact packing mode versus **2** after the dehydration of five water molecules. The new interaction mode gives a dramatic impact on the luminescence properties that cause red shifts of emission spectra due to the excimer emission formation.<sup>30-32</sup> Noteworthy, as the mode of molecular packing has been proved to be influential on the solid-state emission, the modification of polymorphs of a luminescent molecule provides an opportunity to investigate the relationship between crystal packing and optical properties.<sup>32</sup> The fluorescent emission intensity of these three complexes all decreases with extending the irradiation time. The gradually diminished fluorescent intensity originates from the spectral overlap between the emission band and the absorption band of the photo-generated viologen radicals. Accompanied with the energy transfer from a fluorophore to a photochromic group, electron transfer takes place from the carboxyl groups to the viologen units. These three D-A complexes all belong to the fluorescent-photochromic dyad systems.<sup>33</sup> For compound **1** and **3**, the decreased emission intensity can be recovered after heating photocolored samples due to charge recombination (Fig.S7, see ESI†).

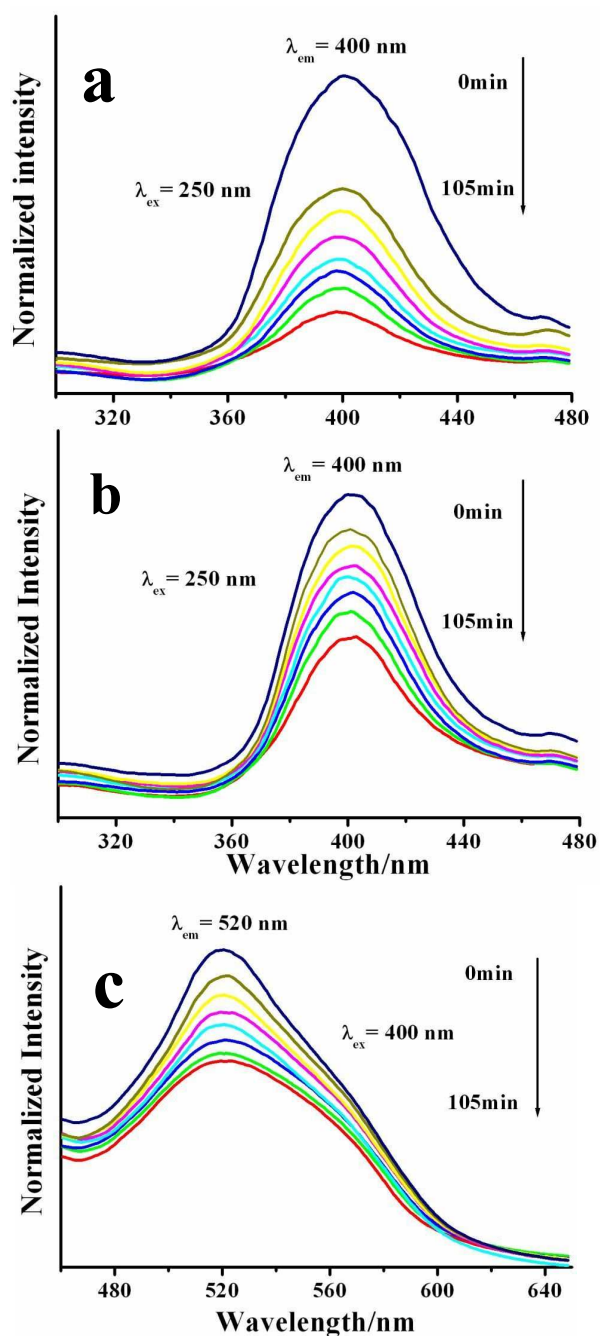


**Fig. 8** Solid-state fluorescent emission spectral changes of the three D-A complexes upon light irradiation: (a) compound **1**; (b) compound **2**; (c) compound **3**.

## Conclusion

As a result of facile synthetic approach, three new crystalline electron transfer type photoactive complexes are prepared *via* the assembly of viologen cations and benzenetetracarboxylate anions. They are characterized by UV-vis, ESR, IR, fluorescence spectra, TGA and PXRD data. A detailed study with regard to the syntheses, structures and photoresponsive characters of the supramolecular D-A assemblies is performed. All of the three complexes are photoactive and can perform a color change under

irradiation. Compound **2** undergoes a solid-state structural transformation to a more compact supramolecular assembly **3** after a dehydration process. Photocolored samples of **1** and **3** can recover to the original state when heated, showing reversible photochromic cycles for at least 5 times. By correlating efficiency of the photosensitive systems with components and structural arrangements, it is concluded that the dissimilar characters can be ascribed to the following factors: (1) the protonation degree of the acceptor units, which affects the generation of radicals, leads to the fact that compound **1** shows the fastest response rate and the highest extent of photoreaction among these three complexes; (2) the distance between the D-A units, which affects the electron transfer process, results in faster photoresponsive characters for **2** than that of **3**. Compound **1**, **2** and compound **3** exhibit fluorescent emission at 400 nm and 520 nm respectively. The red shift of the emission wavelength of **3** can be attributed to the changes of molecular packing. Supramolecular assembly is a useful strategy for obtaining desired D-A photoactive crystals. Understanding the assembly characteristics may throw light on controlling the intermolecular interactions and structural arrangement in the molecular level and manipulating their photoactive properties.

## Acknowledgement

The authors thank the program for NCET (130209), the Project on Integration of Industry, Education and Research of Guangdong Province (2012B091100430), the Fundamental Research Funds for the Central Universities (2014GD0004) and SRP program for financial support, and Mr. Zhang (Analytical and testing center of SCUT) for the collection of crystal data.

## Notes and references

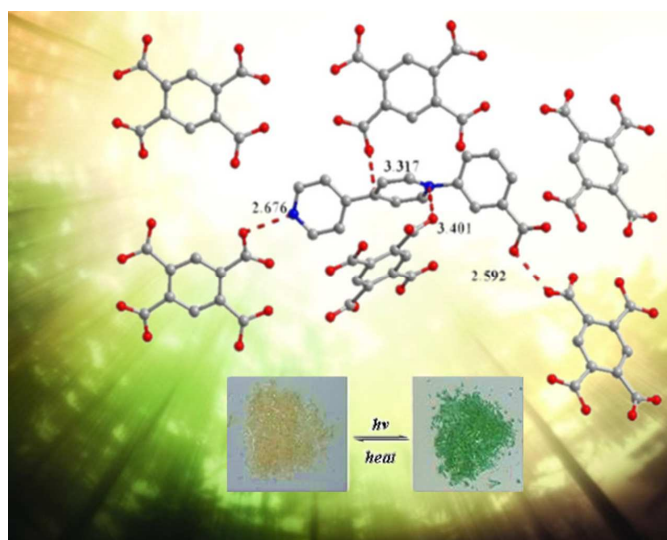
- <sup>a</sup> Key lab for fuel cell technology of Guangdong Province, Guangdong, School of Chemistry and Chemical Engineering, South China University of Technology, Guangzhou, 510640, China. Fax: (+86) 20 8711-2965; Email: zylfu@scut.edu.cn.
- <sup>b</sup> Institute of Materials Physical Chemistry, Huaqiao University, Quanzhou, Fujian, 362021, China. Fax: (+86) 595 2269-0569; E-mail: jcdai@hqu.edu.cn.
- †Electronic Supplementary Information (ESI) available: additional figures, IR spectra, ESR spectra, the calculation of kinetic rate constants and PXRD data. See DOI: 10.1039/b000000x/
- M. D. Ward, *Chem. Soc. Rev.*, 1997, **26**, 365.
  - J. L. Sessler, J. Jayawickramarajah, A. Gouloumis, T. Torres, D. M. Guldi, S. Maldonado and K. J. Stevenson, *Chem. Commun.*, 2005, 1892.
  - A. N. Macpherson, P. A. Liddell, S. Lin, L. Noss, G. R. Seely, J. M. DeGraziano, A. L. Moore, T. A. Moore and D. Gust, *J. Am. Chem. Soc.*, 1995, **117**, 7202.
  - D. D. He, Y. R. Peng, H. Q. Yang, D. D. Ma, Y. H. Wang, K. Z. Chen, P. P. Chen and J. F. Shi, *Dyes Pigments*, 2013, **99**, 395.
  - T. Honda, T. Nakanishi, K. Ohkubo, T. Kojima and S. Fukuzumi, *J. Am. Chem. Soc.*, 2010, **132**, 10155.
  - T. Kuwabara, H. Guo and H. Orii, *Tetrahedron Lett.*, 2012, **53**, 5099.
  - M. Hariharan, J. Joseph, D. Ramaiah, *J. Phys. Chem. B*, 2006, **110**, 24678.
  - M. Ogawa, B. Balan, G. Ajayakumar, S. Masaoka, H. B. Kraatz, M. Muramatsu, S. Ito, Y. Nagasawa, H. Miyasaki and K. Sakai, *Dalton Trans.*, 2010, **39**, 4421.
  - H. Tahara, H. Yonemura, S. Harada, A. Nakashima and S. Yamada, *Chem. Phys. Lett.*, 2012, **42**, 524.

- 10 (a) W. Yu, X. Y. Wang, J. Li, Z. T. Li, Y. K. Yan, W. Wang and J. Pei, *Chem. Commun.*, 2013, **49**, 54; (b) S. Roy, S. P. Mondal, S. K. Ray and K. Biradha, *Angew. Chem. Int. Ed.*, 2012, **51**, 12012; (c) Z. Y. Fu, J. Zhang, Y. Zeng, Y. Tan, S. J. Liao, H. J. Chen and J. C. Dai, *CrystEngComm*, 2012, **14**, 786. (d) Z. W. Chen, G. Lu, P. X. Li, R. G. Lin, L. Z. Cai, M. S. Wang and G. C. Guo, *Cryst. Growth Des.*, 2014, **14**, 2527.
- 11 (a) S. Fukuzumi, K. Ohkubo, F. D'Souza and J. L. Sessler, *Chem. Commun.*, 2012, **48**, 9801; (b) S. Fukuzumi, T. Honda, K. Ohkubo and T. Kojima, *Dalton Trans.*, 2009, **20**, 3880.
- 12 N. Leblanc, W. Bi, N. Mercier, P. Auban-Senzier and C. Pasquier, *Inorg. Chem.*, 2010, **49**, 5824.
- 13 Tetsuo Kuwabara, Haocheng Guo, Hiroki Orii, *Tetrahedron Lett.*, 2012, **53**, 5099.
- 14 Tatsuhiko Honda, Tatsuaki Nakanishi, Kei Ohkubo, Takahiko Kojima, Shunichi Fukuzumi, *J. Am. Chem. Soc.*, 2010, **132**, 10155.
- 15 (a) Y. Zeng, Z. Y. Fu, H. J. Chen, C. C. Liu, S. J. Liao and J. C. Dai, *Chem. Commun.*, 2012, **48**, 8114; (b) T. B. Faust and D. M. D'Alessandro, *RSC Adv.*, 2014, **4**, 17498.
- 16 N. Leblanc, M. Allain, N. Mercier and L. Sanguinet, *Cryst. Growth Des.*, 2011, **11**, 2064.
- 17 (a) M. Irie, *Chem. Rev.*, 2000, **100**, 1685; (b) K. Hakouk, O. Oms, A. Dolbecq, J. Marrot, A. Saad, P. Mialane, H. E. Bekkachi, S. Jobic, P. Deniard and R. Dessapt, *J. Mater. Chem. C*, 2014, **2**, 1628.
- 18 C. C. Ko and V. W. W. Yam, *J. Mater. Chem.*, 2010, **20**, 2063.
- 19 (a) J. Cusido, E. Deniz, and F. M. Raymo, *Eur. J. Org. Chem.*, 2009, 2031; (b) J. Guo, D. Jia, L. Liu, H. Yuan and F. Li, *J. Mater. Chem.*, 2011, **21**, 3210.
- 20 D. Bongard, M. Moller, S. N. Rao, D. Corr and L. Walder, *Helv. Chim. Acta*, 2005, **88**, 3200.
- 21 G.M. Sheldrick, SHELXTL, version 5.1; Bruker Analytical X-ray Instruments Inc., Madison, Wisconsin, 1998.
- 22 G. M. Sheldrick, SHELXS-97, PC version; University of Göttingen, Göttingen, Germany, 1997.
- 23 (a) T. Yui, Y. Kobayashi, Y. Yamada, K. Yano, Y. Fukushima, T. Torimoto and K. Takagi, *ACS Appl. Mater. Interfaces*, 2011, **3**, 931; (b) Q. L. Zhu, T. L. Sheng, R. B. Fu, S. M. Hu, L. Chen, C. J. Shen, X. Ma and X. T. Wu, *Chem. Eur. J.*, 2011, **17**, 3358.
- 24 T. Miura, *J. Phys. Chem. B*, 2013, **117**, 6443.
- 25 H. Yoshikawa, S. Nishikiori, T. Watanabe, T. Ishida, G. Watanabe, M. Murakami, K. Suwinska, R. Luboradzki and J. Lipkowski, *Dalton Trans.*, 2002, 1907.
- 26 (a) J. K. Sun, L. X. Cai, Y. J. Chen, Z. H. Li and J. Zhang, *Chem. Commun.*, 2011, **47**, 6870; (b) Y. Zeng, Z. Y. Fu, H. J. Chen, C. C. Liu, S. J. Liao and J. C. Dai, *Chem. Commun.*, 2012, **48**, 8114.
- 27 P. C. Jhang, N. T. Chuang and S. L. Wang, *Angew. Chem. Int. Ed.*, 2010, **49**, 4200.
- 28 J. K. Sun, P. Wang, Q. X. Yao, Y. J. Chen, Z. H. Li, Y. F. Zhang, Y. M. Wu and J. Zhang, *J. Mater. Chem.*, 2012, **22**, 12212.
- 29 (a) R. G. Lin, G. Xu, M. S. Wang, G. Lu, P. X. Li and G. C. Guo, *Inorg. Chem.*, 2013, **52**, 1199. (b) N. Mercier, *Eur. J. Inorg. Chem.*, 2013, 19.
- 30 H. Y. Zhang, Z. L. Zhang, K. Q. Ye, J. Y. Zhang and Y. Wang, *Adv. Mater.*, 2006, **18**, 2369.
- 31 E. Q. Procopio, M. Mauro, M Panigati, D. Donghi, P. Mercandelli, A. Sironi, G. D'Alfonso and L. D. Cola, *J. Am. Chem. Soc.*, 2010, **132**, 14397.
- 32 (a) Y. Fan, Y. F. Zhao, L. Ye, B. Li, G. D. Yang and Y. Wang, *Cryst. Growth Des.*, 2009, **9**, 1421; (b) Y. Fan, W. F. Song, D. Y. Yu, K. Q. Ye, J. Y. Zhang and Y. Wang, *CrystEngComm*, 2009, **11**, 1716; (c) C. H. Shin, J. O. Huh, M. H. Lee and Y. Do, *Dalton Trans.*, 2009, **33**, 6476.
- 33 (a) I. Yildiz, E. Deniz and F. M. Raymo, *Chem. Soc. Rev.*, 2009, **38**, 1859; (b) Y. Hasegawa, T. Nakagawa and T. Kawai, *Coord. Chem. Rev.*, 2010, **254**, 2643; (c) Y. Zeng, S. J. Liao, J. C. Dai and Z. Y. Fu, *Chem. Commun.*, 2012, **48**, 11641.

## GRAPHICAL ABSTRACT

**Molecular packing, crystal to crystal transformation, electron transfer behaviour, photochromic and fluorescent property of three hydrogen-bonded supramolecular complexes containing benzenecarboxylate donors and viologen acceptors**

Hengjun Chen,<sup>a</sup> Min Li,<sup>a</sup> Guiming Zheng,<sup>a</sup> YiFang Wang,<sup>a</sup> Yang Song,<sup>a</sup>  
Conghui Han,<sup>a</sup> Zhiyong Fu<sup>\*a</sup> Shijun Liao,<sup>a</sup> and Jingcao Dai<sup>b</sup>



An investigation into the relation between structures of three D-A supramolecular systems and their photoresponsive characteristics is presented. Compound **1** [H<sub>2</sub>CPBPY] [H<sub>2</sub>BTEC] and compound **2** [HCPBPY]<sub>2</sub>·[H<sub>2</sub>BTEC]·5H<sub>2</sub>O are prepared with the same starting materials at different pH values and characterized by single crystal X-ray diffraction, powder X-ray diffraction, UV, IR and ESR spectra. Electron-deficient CPBPY moieties and electron-donating BTEC units are linked by hydrogen-bonds and  $\pi$ - $\pi$  stacking interactions to form the donor-acceptor system. Under light irradiation, photoactivated electrons can transfer from the donor to the acceptor units in both **1** and **2**, giving rise to a long-lived charge-separated state and accompanying with an interesting color changing phenomenon. Crystals of **2** allowed to dehydrate at elevated temperatures undergo single-crystal to single-crystal transformation to yield **3** [HCPBPY]<sub>2</sub>·[H<sub>2</sub>BTEC], accompanied by a drastic change in structural arrangements. For the photocoloration character, compound **1** shows a faster photoresponsive rate than **2** and **3**. For the fluorescence property, compound **1** and **2** all exhibit photoluminescence emission centered at 400 nm, whereas **3** exhibits photoluminescence emission at 520 nm, showing a significant red shift of 120 nm. Their different photoactive characters can be attributed to the connecting, packing modes and the valence states of the functional D-A moieties.